Hyperspectral characterization of an in vitro wound model

Lise L. Randeberg[a], Janne-Lise Hegstad[a], Lukasz Paluchowski[a], Matija Milanic[a], Brita S. Pukstad[a,b]

[a] Norwegian University of Science and Technology, Trondheim, Norway.
[b] St. Olav's Hospital, Trondheim, Norway

ABSTRACT

Wound healing is a complex process not fully understood. There is a need of better methods to evaluate the different stages of healing, and optical characterization is a promising tool in this respect. In this study hyperspectral imaging was employed to characterize an in vitro wound model. The wound model was established by first cutting circular patches of human abdominal skin using an 8 mm punch biopsy tool, and then creating dermal wounds in the center of the skin patches using a 5 mm tool. The wounds were incubated in medium with 10% serum and antibiotics. Hyperspectral images were collected every three days using a push broom hyper spectral camera (Hyspex VNIR1600). The total measurement period was 21 days. The camera had a spectral resolution of 3.7 nm and was fitted with a close up lens giving a FOV of 2.5 cm and a spatial resolution of 29 μm. Data were processed in ENVI and Matlab. The healing zone in the in vitro model could not be easily visually identified without dying. A successful classification of the hyperspectral data using the Spectral Angle Mapping (SAM) is presented. The hyperspectral results showed that newly formed epithelium could be imaged without any additional contrast agents or dyes. It was also possible to detect non-viable tissue due to spectral changes. In vitro wound models and hyperspectral imaging can thus be employed to gain further insight in the complicated process of healing in different kinds of wounds.

Keywords: Hyperspectral imaging, Dermatology, Imaging spectroscopy, Dermatology, Chronic wounds, Tissue optics, Skin

1. INTRODUCTION

Wound healing is a complex process that is not fully understood. Further understanding is needed to be able to provide the best possible treatment for acute wounds, burns, and chronic wounds of any kind. Some of the needed basic research in this area is difficult to carry out in vivo. In vitro models might thus be a convenient tool and contribute to an increased understanding of the different stages of healing. A standardized and repeatable in vitro model of acute wounds has been developed by Kratz *et al.* [1]. In their model skin from breast reduction surgery was cut into circular wounds with a diameter of 6 mm, and wound with a diameter of 3 mm was created in the middle of the sample. The model was followed for 14 days and the re-epithelialization process was studied by taking out samples for histology and immunohistochemical evaluation. Jansson *et al.* [2] studied the re-epithelialization occurring in such skin models. They found that the healing process seen in the model is similar to the healing in a real wound provided that the wound surface of the samples is exposed to air.

Jansson *et al.* and Kratz *et al.* used histology and immunochemistry to study the healing process. They could not follow the same wound throughout the study period as the testing is destructive. This is a drawback of the model as there might be differences between the samples. Optical techniques might in this case provide a non-destructive, non-contact method for sample evaluation that allows for following the same sample throughout the study period.

Hyperspectral imaging is a non-contact technique that combines high spectral and spatial resolution and allows for spectroscopic and statistical evaluation of the samples. Hyperspectral imaging has been proved to

Correspondence to L.L.R.:
Department of Electronics and Telecommunications, Norwegian University of Science and Technology,
N-7491 Trondheim, Norway
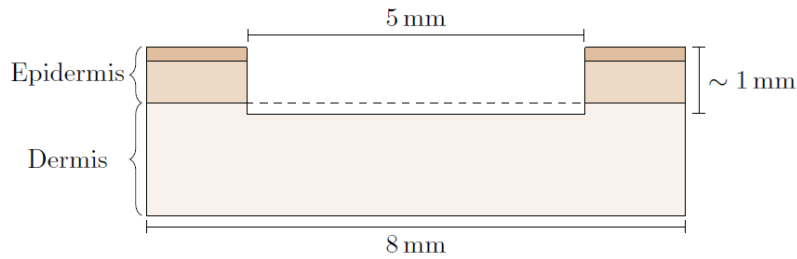E-mail: Lise.Randeberg@iet.ntnu.no
Fax: +47 73591441

Figure 1. Cross section of a wound model.

have a potential for medical diagnostics. A nice review of both the technology and medical applications can be found in [3].

The non-contact nature of this technique makes it possible to follow each sample independently throughout the experiment. The re-epithelialization can be assumed to affect the optical properties of the sample, and it should thus be possible to monitor the healing using hyperspectral imaging.

The aim of this study was to implement a modified version of Kratz' skin model and to investigate if hyperspectral imaging in the visible spectral range can be used to monitor the re-epithelialization of in vitro wounds as a function of time. The wounds created in this project were followed for a total of 21 days and data were collected every third day. The data were classified using the spectral angle mapper (SAM).

2. THEORY AND METHODS

2.1. Wound model

The in vitro wound model was made from human abdominal skin collected during plastic surgery. The skin used in this study originated from one donor. The project was approved by the regional ethical committee (REK-Midt-Norge). The design of the models is a modified version of the design presented by [1], see Fig. 1.

In the present study a 8 mm punch biopsy tool was used to create circular full depth cuts in the donor skin. The wound was made in the center of the 8 mm skin patch by applying a 5 mm punch biopsy tool to define the circumference of the wound. This cut protruded through the epidermis and into the dermis without being a full thickness cut. The 5 mm centerpiece was lifted from the surface using a syringe and then cut using a scalpel. Finally, the model was removed from the larger donor skin patch by lifting it with a pair of forceps and cutting it lose. Any remains of subcutaneous fat was removed before the models were placed in the growth medium.

The models were kept in Dulbecco's Modified Eagle Medium (DMEM) with 10% fetal calf serum (FCS), 50 μg/ml penicillin, streptomycin 50 U/ml and glutamin added. The models were kept floating in the medium with the wound surface exposed to air, see Fig. 2. Air exposure of the surface is important to ensure epitheialization in more than one layer [2]. The samples were incubated at 37°C and in an atmosphere containing 5% CO_2 (Forma Steri-Cycle CO_2 incubator, Thermo Scientific, Waltham, Massachusetts, USA).

Hyperspectral data were collected every three days for 21 days in total. Samples for histology were collected every third day. However, these results will not be presented in this paper. The growth medium was changed every three days as well.

2.2. Re-epitalialization of wounds

A wound occurs when the epidermis is damaged. Re-epitalialization is the process of regenerating the missing epithelial tissue. This process occurs by migration of keratinocytes from the edge of the surrounding epidermis. The keratinocytes migrate from the deeper layers of the epidermis and into the open area of the wound. This is a complex process involving keratinocytes, fiberoblasts and immune cells. The description of this process given in this paragraph is taken from Arnoux, Jansson and Myers [2, 4, 5]. The first phase of healing of a wound is the coagulation phase where fibrin and blood platelets produce a blood clot that covers the wound. This phase is
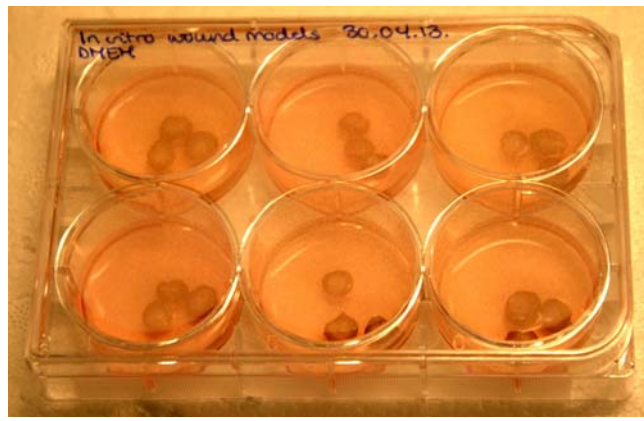
Figure 2. Skin models floating in growth medium

followed by an inflammatory phase with infiltration of leukocytes, followed by macrophages. In the granulation phase new tissue starts to form to heal the wound. This is a complex phase involving several types of cells and signaling agents. The re-epitheliaization occurs when the wound cavity has been filled with granulation tissue. In that phase a healing edge of migrating keratinocytes can be found in the wound. It has been shown that there is just one layer of cells migrating from the edge toward the center of the open wound. When the entire wound surface is covered by keratinocytes they will start to divide and create a thicker epithelial layer covering the wound [2]. Finally, new connective tissue is formed and the wound will be contracted.

2.3. Skin optical properties and hyperspectral imaging

Hyperspectral data are images of the surface radiance of an object. The data contains a full spectrum in each pixel, and can be converted to reflectance images by calibrating the scene against a standard with known reflectance properties. Each pixel in the image will then contain a full reflectance spectrum that can be further analyzed using either statistical methods like image analysis, or by spectroscopic techniques.

Minima in measured skin reflectance are due to characteristic peaks in the absorption spectra of apparent chromophores. See Fig. 3 for absorption spectra of common chromophores in normal skin. Hemoglobin is one of the most important absorbers in skin, however, in this study only some traces of blood could be observed in a few samples. The most important chromophores are thus expected to be melanin (in the intact skin), lipids and water. The melanin absorption decreases exponentially with wavelength [6, 7], and will thus affect the steepness of the reflectance curve across the visible spectral range. The water absorption is low in the visible spectral range, the most prominent absorption peak is at $970-980$ nm [8]. Other absorbers like lipids, bilirubin and betacarotene are also present in tissue. Lipids absorb around 480 nm and 930 nm, while betacarotene and bilirubin absorbs in the blue green spectral range with peaks at 480 and 460 nm, respectively [9, 10, 11].

Due to the lack of hemoglobin absorption, it might be possible to observe absorption in cytochromes. This absorption is usually masked by the hemoglobin absorption in in vivo skin due to the relatively higher hemoglobin concentration. Cytochromes are hemeproteins found in mitochondria, where they are bound to the inner membrane. The cytochromes generate ATP via the electron transport and is thus essential for the cell metabolism. Due to the heme groups they exhibit absorption in the VIS-NIR spectral range. Cytochrome absorption will depend on the redox status of the molecule and will thus vary with the metabolic status of the tissue. A figure of the absorption spectra of cytochrome-b and -c can be seen in Fig. 4.

The scattering in skin is caused by scattering from blood cells (which will be a marginal contribution in this study), other cells and cell organelles as well as lipid droplets and collagen fibers. This gives rise to a combination of Mie- and Rayleigh scattering that decreases monotonically with increasing wavelength [14].

All measurements in this study were performed using a hyperspectral camera system developed by Norsk Elektro Optikk AS (HySpex VNIR 1600 ($400-1000$ nm), Norsk Elektro Optikk AS, Lørenskog, Norway).
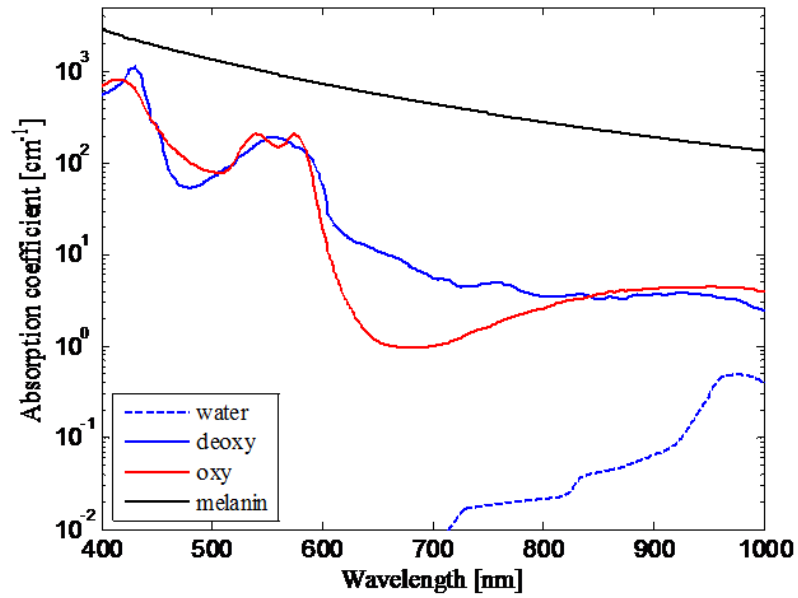
Figure 3. Absorption of the most common chromophores in human skin. Oxy- and deoxyhemoglobin [12], melanin [6, 7], and water [8].
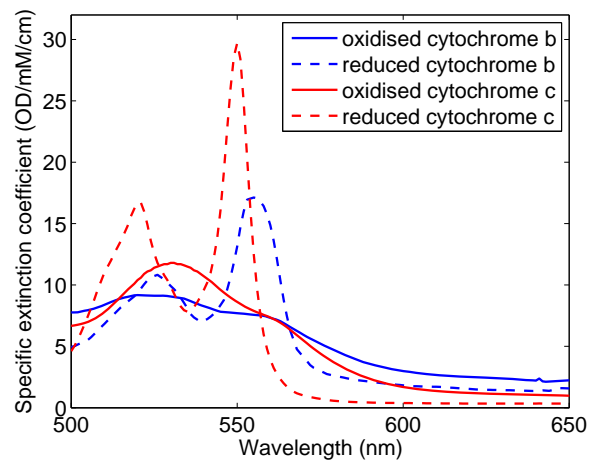

Figure 4. Absorption spectra of cytochrome-b and -c. Data from [13].

Table 1. System specifications for the Hyspex hyperspectral camera.

Module	VNIR-1600
Detector	Si CCD (1600 × 1200)
Spectral range	$0.4 - 1.0 \ \mu$m
Spatial pixels	1600
FOV across track	$17°$
Pixel FOV across/along track	0.2 mrad/0.4 mrad
Spectral sampling	3.7 nm
No. of spectral bands	160
Digitization	12 bit
Frame rate to HD	$\geq$ 120 fps

For the measurements performed in this study the camera was fitted with a focusing lens with a working distance of 5 cm, and a field of view (FOV) of about 2.5 cm. The spatial resolution at the sample surface was about 30 μm. See Table 1 for system specifications. The hyperspectral images were collected using a cross polarized setup with polarizers (VersaLight wire grid polarizers, VLR100-NIR, Laser Physics UK Ltd, Milton Green, Cheshire, U.K.) fitted to both the camera lens and the light source. This was done to avoid specular reflection from the skin surface. A broad band DC light source was applied for the measurements (DCR III, Schott Fostec, Auburn, New York, USA).

2.4. Data analysis

Data were analyzed using ENVI 4.8 (Exelis Visual Information Solutions, Crowthorne, Berkshire, U.K.) and Matlab (The MathWorks Inc., Nordic Offices, Kista, Sweeden). Reflectance images were created by calibrating the radiance data against a Spectralon tile (Ocean Optics, Duiven, The Netherlands). Reflectance spectra were collected from the images to analyze the temporal change in the samples. The minimum noise fraction transform (MNF) [15, 16], was used for noise reduction.

Spectral angle mapping (SAM) was used for supervised classification of the normal, intact skin surface, the healing zone and the wound area. Regions of interest (ROIs) were selected from the samples at day 3 and the average spectra from these ROIs were used as input spectra for the classification. The spectral angle mapper is known to be relatively insensitive to intensity variations across the imaged scene. Following the SAM classification class statistics were used to compute the average spectra of each class in the image.

3. RESULTS AND DISCUSSION

3.1. Spectral data

Spectra extracted from the hyperspectral data from day 3 are used as the baseline data for the classification. This was done because the data from day 1 were impossible to use due to specular reflection from the sample surface and the containers. Crossed polarizers were fitted to the system before the measurements at day 3, this reduced the amount of specular reflection. However, specular reflection from the plastic containers and from the moist and uneven surface was not completely eliminated by the introduction of the polarizers, and it remained a problem throughout the measurement period.

The fact that day 3 is used as the baseline might have affected the results slightly, but not the conclusion. At that point in time the wounds had started to heal, but were far from completely healed.

Figure 5 shows the change in the average spectra of the intact skin, healing edge and wound as a function of time. At day 3 the spectra are relatively far from each other. The intact skin exhibits the lowest reflectance values, and the wound the highest values while the edge lies in between. This can probably be due to several factors. The intact skin contains melanin which will lead to a lower reflectance. It is also to be expected that there is a difference in scattering properties in these regions. Both those effects are wavelength dependent and affect shorter wavelengths the most. Specular reflection is not strongly wavelength dependent, and it seems like
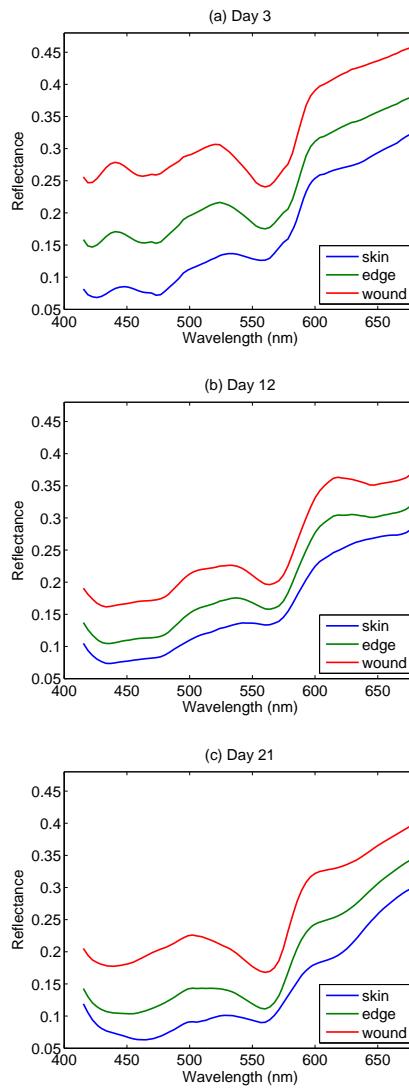
Figure 5. Temporal development of average spectra from the intact skin, healing edge and wound. From top: day 3; day 12; day 21.

that might be an important reason for the high reflection seen from the open wound. The edge spectra are getting closer to the intact skin spectra with time, especially for shorter wavelengths, while the open wound does not approach the other spectra significantly.

The spectral changes described above are expected differences between the skin, edge and wound. These changes can be explained by changes in scattering and melanin absorption. Figure 6 shows spectra from the different parts of the wound as a function of time. These spectra show changes that can be explained by altered scattering properties and melanin content. However, the spectra exhibit a wavelength shift that cannot be explained by the most common skin chromophores. Reflectance minima are found at 560 nm and 620 nm. These minima are shifted toward longer wavelengths with time and the minimum around 620 nm becomes more pronounced. This effect is especially visible at day 21. It can bee seen in all parts of the sample, but is most prominent in the wound.

One possible source of error might be the growth medium the samples were floating in. The color of the medium was found to change from pink to a more pale yellowish hue as the samples extracted nutrition from
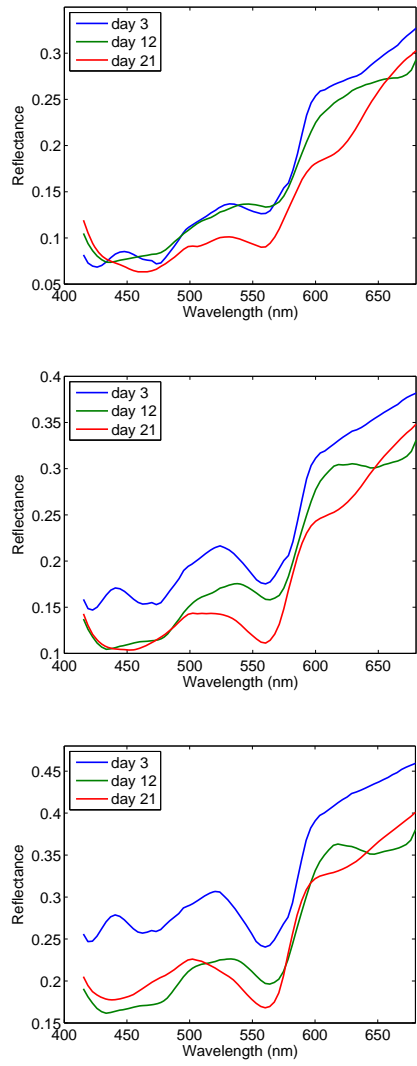
Figure 6. Temporal development of spectra at days 3, 12 and 21. From top: intact skin; healing edge; wound.
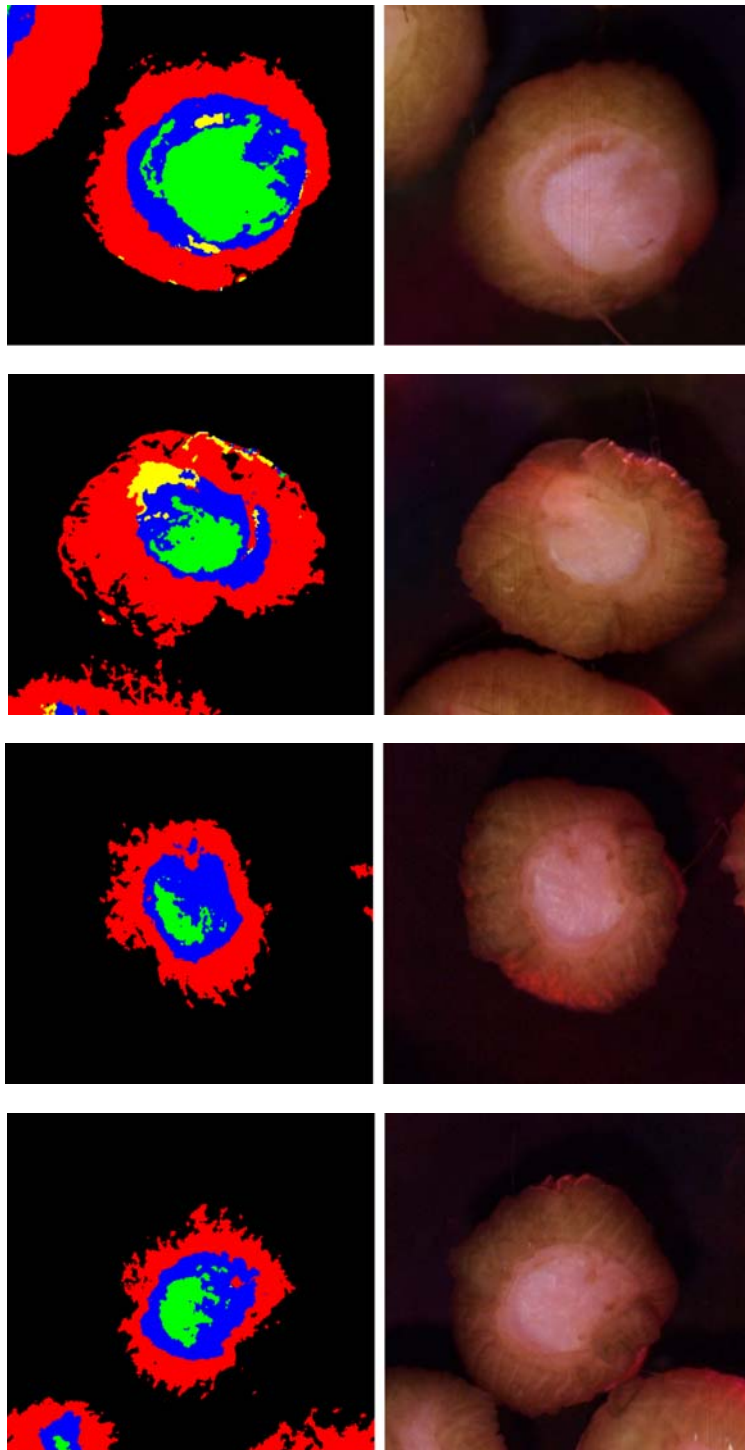
Figure 7. Temporal development of a typical sample. Left column: SAM classification based on spectra from day 3. Red indicates intact skin, blue is the healing zone and green is the open wound. The yellow class is unknown. From top: day 3; day 9; day 18; day 21. Right column: RGB images, same order as in the left column.
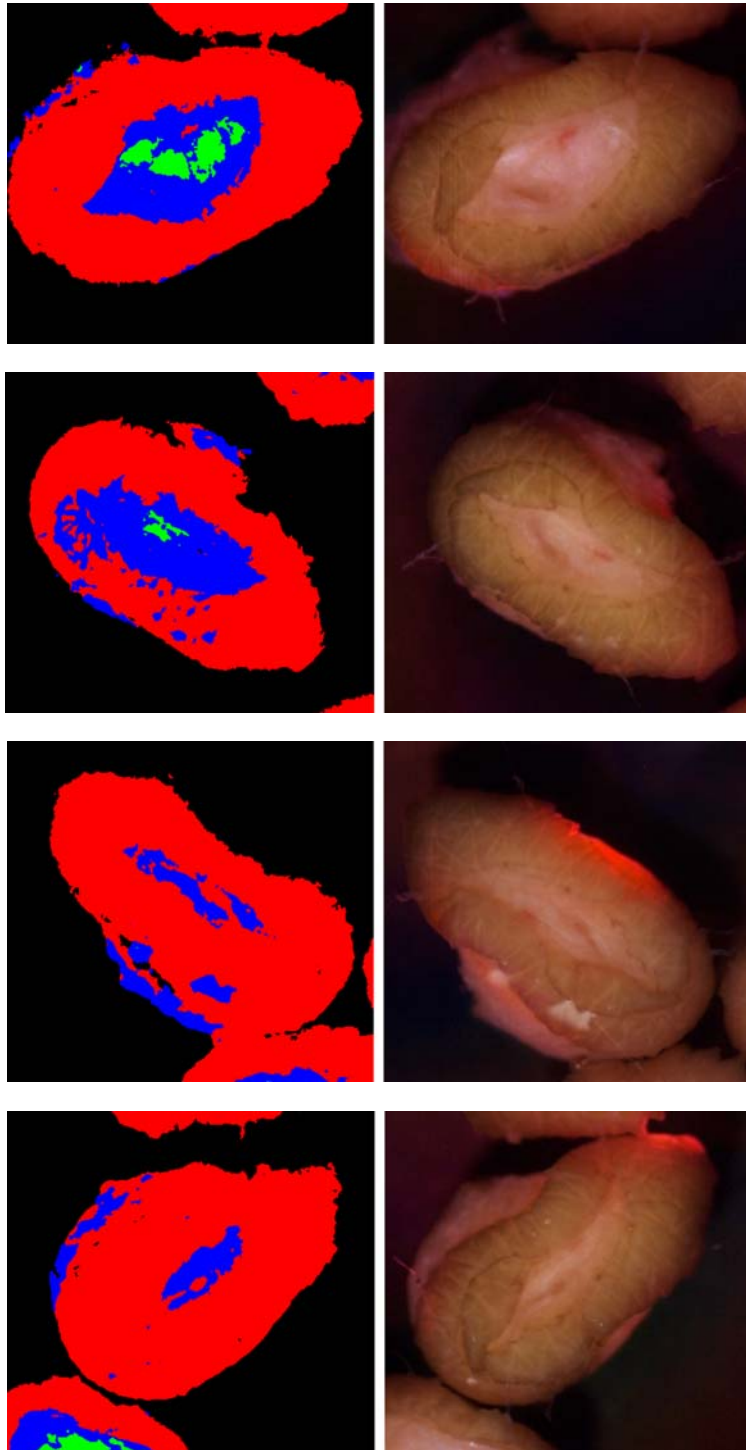
Figure 8. Temporal development of a sample with a large degree of contraction. Left column: SAM classification based on spectra from day 3. Red indicates intact skin, blue is the healing zone and green is the open wound. From top: day 3; day 9; day 18; day 21. Right column: RGB images, same order as in the left column.

it. This change in medium color might have affected the measured spectra, however, the medium was always changed at the same time with respect to the measurements. It is therefore not considered as a the most probable cause for the observed spectral changes.

Some of the observed spectral shifts might be caused by changes in the redox state of the present cytochromes, see Fig. 4. It should be mentioned that he samples included in this study were kept for 21 days before the experiment was ended. At that point in time the samples were dead. As a comparison Kratz [1] kept their model running for 14 days. The presented results must be considered as preliminary, and the study will have to be repeated to see if the same effect occurs. This idea will be further investigated in future work.

3.2. SAM classification

Figures 7 and 8 show SAM classification of two samples on days 3, 9, 18 and 21. The intact skin, healing zone and open wound can clearly be identified based on the classification. Based on these results it can be concluded that SAM seems to be a promising method to monitor healing in this model. It can be seen from the images that the healing is progressing symmetrically from the edge of the wounds as described by Kratz and Jansson [1, 2]. The wound model shown in Fig. 8 shows contraction of the wound area. This wound was observed to be completely covered by epithelium at day 21. In this case the shape of the wound is totally altered. The change in shape makes it impossible to coregister the wounds for further image analysis.

This study has presented data showing that hyperspectral imaging is a convenient tool to monitor this specific in vitro skin model. The healing can easily be monitored in a non-destructive manner. The approach can be extended to other models, and it can be used to monitor this model under different conditions. Future work will include repeating the experiments shown in this study, and extending them to measuring more complex systems. It might be of interest to observe the effect of infection or the impact of various pharmaceutical compounds.

4. CONCLUSION

This study shows that hyperspectral imaging is a suitable tool for non-destructive monitoring of in vitro wounds. The healing of the wounds could be observed both through classification using the spectral angle mapping technique and through inspection of the reflectance spectra. The healing zone could be easily visualized by the classification results. As the presented model is an in vitro system without considerable blood, the changes in cytochrome redox status might be monitored, and the loss of samples may be predicted from the spectral behavior before the samples can be visually observed to be dead.

ACKNOWLEDGMENTS

References

[1] G. Kratz, "Modeling of wound healing processes in human skin using tissue culture," *Microsc Res Techniq* **42**(5), pp. 345–350, 1998.

[2] K. Jansson, G. Kratz, and A. Haegerstrand, "Characterization of a newin vitro model for studies of reepithelialization in human partial thickness wounds," *In Vitro Cell Dev-An* **32**(9), pp. 534–540, 1996.

[3] G. Lu and B. Fei, "Medical hyperspectral imaging: a review," *J Biomed Opt* **19**(1), p. 010901, 2014.

[4] V. Arnoux, C. Come, D. Kusewitt, L. Hudson, and P. Savagner, "Cutaneous wound reepithelialization," in *Rise and Fall of Epithelial Phenotype, Molecular Biology Intelligence Unit*, pp. 111–134, Springer US, 2005.

[5] S. R. Myers, I. M. Leigh, and H. Navsaria, "Epidermal repair results from activation of follicular and epidermal progenitor keratinocytes mediated by a growth factor cascade," *Wound Repair Regen* **15**(5), pp. 693–701, 2007.

[6] R. R. Anderson and J. A. Parrish, "The optics of human skin," *J Invest Dermatol* **77**(1), pp. 13–19, 1981.

[7] M. L. Wolbarsht, A. W. Walsh, and G. George, "Melanin, a unique biological absorber," *Appl Opt* **20**, pp. 2184–2186, 1981.

[8] G. M. Hale and M. R. Querry, "Optical constants of water in the 200 nm to 200 μm wavelength region," *Appl Opt* **12**, pp. 555–563, Mar 1973.

[9] H. Du, R. A. Fuh, J. Li, A. Corkan, and J. S. Lindsey, "PhotochemCAD: A computer-aided design and research tool in photochemistry," *Photochem Photobiol* **68**, pp. 141–142, 1998.

[10] L. L. Randeberg, A. J. Daae Hagen, and L. O. Svaasand, "Optical properties of human blood as a function of temperature," *Proceedings of SPIE* **4609**, pp. 20–29, 2002.

[11] M. B. Lilledahl, O. A. Haugen, M. Barkost, and L. O. Svaasand, "Reflection spectroscopy of atherosclerotic plaque," *J Biomed Opt* **11**(2), pp. 021005–021005–7, 2006.

[12] M. Friebel, A. Roggan, G. Muller, and M. Meinke, "Determination of optical properties of human blood in the spectral range 250to1100nm using monte carlo simulations with hematocrit-dependent effective scattering phase functions," *J Biomed Opt* **11**(3), pp. 034021–034021–10, 2006.

[13] U. D. o. M. P. Biomedical Optics Research Laboratory and Bioengineering. `http://www.ucl.ac.uk/medphys/research/borl/intro/spectra`. Accessed January 2014.

[14] S. L. Jacques, "Optical properties of biological tissues: a review," *Phys Med Biol* **58**(11), p. R37, 2013.

[15] A. A. Green, M. Berman, P. Switzer, and M. D. Craig, "A transformation for ordering multispectral data in terms of image quality with implications for noise removal," *IEEE Transactions on Geoscience and Remote Sensing* **26**(1), pp. 65–74, 1988.

[16] J. W. Boardman and F. A. Kruse, "Automated spectral analysis: a geological example using aviris data, north grapevine mountains, nevada," *Proceedings of ERIM Tenth Thematic Conference on Geologic Remote Sensing* , pp. 407–418, 1994.